

Molecular folds in polyethylene observed by atomic force microscopy*

Rajkumari Patil and Darrell H. Reneker†

Maurice Morton Institute of Polymer Science, The University of Akron, Akron, OH 44325-3909, USA

(Received 2 August 1993; revised 20 September 1993)

Folded chain lamellar crystals of polyethylene were examined by atomic force microscopy. Particular care was taken to ensure that the areas examined at high magnification were on the fold-containing surface of the crystals. High spots observed on this surface formed a 2D array. The spacings and angles of the array were consistent with the positions expected for the folds when viewed from a direction perpendicular to the fold-containing surface and were not the same as expected if viewed along the chain axis. Spacings appropriate for the usual orthorhombic unit cell and for the monoclinic unit cell that can be produced by mechanical deformation were observed. Local variations in the shape and position of the spots indicate that folds of different orientation and structure were present. In many observations of similar fold surfaces at high magnification, only images of lower quality which did not show the periodic arrays of spots were observed. Reasons for the images without periodic order are proposed.

(Keywords: polyethylene; lamellar crystals; folded chains)

INTRODUCTION

The new results presented here show that atomic force microscopy (AFM) can be used to image directly the arrangements of the folds on the surfaces of polymer folded chain lamellar crystals, and also provide morphological information about irregularities that may be present. Molecular folding of synthetic polymer molecules was deduced as a general and pervasive phenomenon from the observation in the late 1950s of lamellar crystals of polyethylene. Crystals of folded polymer molecules have been described in monographs by Geil¹, Bassett², Mandelkern³ and Wunderlich⁴. Since direct evidence about the arrangement of folds was sparse^{5,6}, a lively scientific discussion of various possibilities has occurred through the past several decades. The 1979 Faraday Discussions of the Chemical Society contains papers dealing with polymer chain folding by Flory^{7,8}, Frank⁹, Hoffman *et al.*¹⁰ and many others.

As the polymer molecules crystallize from solution or from the molten phase, they adopt a planar zigzag or other helical conformation as they attach to the edges of growing lamellar crystals. These straight segments, often called stems, lie along a direction that has a large component parallel to the normal to the lamellar surface. The lamellae are typically only 10 nm thick, so the polymer molecules, which are much longer, fold at the surface of the lamellae by appropriate rotations around bonds, and form a set of stems in the crystal.

Modifications, during processing, of the patterns of folding affect the mechanical and other physical properties. The conformation of the folds, the arrangements

of the stems in the lamella, the directions and paths that the folds take to connect the stems and other such questions are of continuing interest. The answers to these questions shed light on crystallization rates, the use of polymer crystals as building blocks of larger structures, and the formation of very high modulus fibres. The ability of an atomic force microscope to produce the images of folds, described in this paper, means that these questions can now be addressed in a straightforward and powerful way. It is also now well established that hydrogen-bonded molecules such as nylon and synthetic polypeptides fold into lamellar crystals. The direct observation of folds is a matter of practical importance in synthetic polymers, and also provides a reference point in addressing the behaviour of protein molecules¹¹⁻¹³. Sequences of amino acid residues that favour molecular folding have been identified in proteins¹⁴. The morphology of the crystalline-frozen liquid crystalline solid state also suggests chain folding¹⁵.

EXPERIMENTAL

Lamellar crystals of linear polyethylene (standard reference material 1475 from the National Institute of Standards and Technology, Gaithersburg, MD; $MW \approx 50\,000$) were grown by a self-seeding technique from a 0.1% dilute solution in xylene. Polyethylene was dissolved in boiling xylene and then precipitated by cooling to form large, complicated, lamellar, dendritic crystals. These crystals were reheated in the xylene until the scattering of a light beam passing through the suspension was greatly reduced. At this point, a large portion of each polymer crystal had redissolved, but many small pieces remained and served as nuclei for the growth of new crystals upon subsequent cooling. The large number of nuclei present competed for the molecules in

* Presented at 'International Polymer Physics Symposium Honouring Professor John D. Hoffman's 70th Birthday', 15-16 May 1993, Washington, DC, USA

† To whom correspondence should be addressed

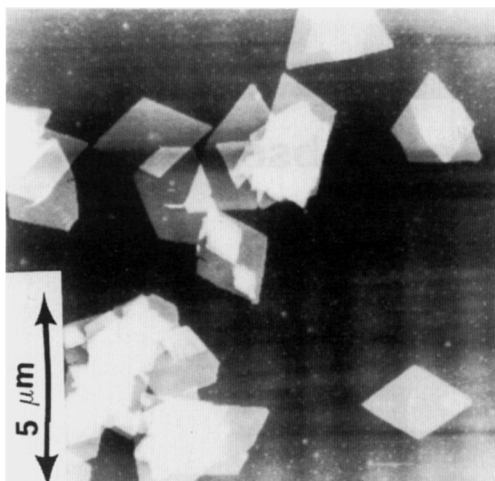


Figure 1 Pyramidal lamellar crystals of polyethylene

solution so that many small, relatively simple lamellar crystals were produced.

The crystals suspended in xylene were sprayed onto a glass slide, dried, shadowed with an evaporated mixture of platinum and carbon, and then floated onto copper grids. The general morphology of the crystals was observed with a transmission electron microscope. Typically, crystals with one lamella a few micrometres across and containing a few growth spirals were observed. These lamellae were mostly lozenge-shaped, hollow pyramids but some crystals had more complicated shapes. Generally, upon solvent evaporation, the hollow pyramids collapsed onto the substrate in such a way as to form pleats along the minor diagonal of the lozenge.

Crystals were also sprayed onto a cleaved mica surface. Surfaces of the collapsed lamellar crystals were then examined with a Digital Instruments Nanoscope II atomic force microscope. Imaging was done at ambient conditions either by using a stiff, triangular cantilever of length $100\ \mu\text{m}$ with a tip force of $5\ \text{nN}$ or a more flexible triangular cantilever of length $200\ \mu\text{m}$ with a tip force of less than $1\ \text{nN}$. All the images were captured while scanning with low gains and without using filters.

OBSERVATIONS AND RESULTS

Figure 1 shows several typical lamellar crystals which were imaged by an AFM scanner with a maximum scan length of $10\ \mu\text{m}$. The characteristic lozenge shapes, growth spirals and, at higher magnifications, ridges along the fold domain boundaries are clearly seen. The measured thickness of these crystals is 11 to 12 nm. Figure 2 shows the thickness of the basal lamella to be 11.5 nm and the thickness of the top layer in the growth spiral to be 10.44 nm. The thickness of the lamellae in a growth spiral terrace is smaller for the higher levels of the terrace, as was described elsewhere for this sample¹⁶.

Transmission electron micrographs as well as atomic force micrographs show pleats along the minor diagonals on some of the crystals, thus confirming the above collapse process. Other collapse features such as pleats along the major diagonal of the lozenge, corrugations parallel to $\{310\}$ and wrinkles are also observed on some of the lamellae. Most collapse modes involved rotation of large areas of the lamellae about a line at the intersection of the $\{110\}$ growth faces with the $\{332\}$

planes. The $\{332\}$ planes are tangential to the chain folds in a common form of the hollow pyramidal crystals¹⁷.

The surfaces of the collapsed crystals were also scanned by using the high resolution scanner of the atomic force microscope. It was usually not possible to observe an entire crystal because the minor diagonal of each crystal measures about $1\ \mu\text{m}$ and the high resolution scanner has a maximum scan length of 800 nm. When recognizable features such as $\{110\}$ growth face, a fold domain boundary or an apex were seen, the lamellar thickness was measured on a section across the growth face such as that shown in Figure 2. Such sets of observations were used to ensure that the scanning tip of the atomic force microscope was on the fold surface of the crystal and not on the mica substrate.

An $800 \times 800\ \text{nm}$ square scan area from one such scan is shown in Figure 3. This figure shows part of a lamellar crystal with $\{110\}$ growth faces (indicated by arrows) which meet at an angle that indicates that the fold domain boundary bisecting them is along the short diagonal of a lozenge-shaped crystal. The basal lamella is 11.5 nm thick, which agrees with the lamellar thickness of the crystals in this sample. The horizontal lines parallel to the scan direction appear after several scans and are similar to those observed occasionally when the AFM tip drags across and mechanically deforms a lamellar crystal.

Molecular-scale images were obtained by scanning smaller areas of the fold surface at higher magnification. An area of about $100\ \text{nm}^2$ on this crystal is shown in Figure 4. A periodic pattern with some noise was observed in repeated scans. The scan rate was set at 8 Hz to minimize noise in this image. The unfiltered data, as is often the case at slow scan rates, contained hills and valleys parallel to the scan lines with the hills separated by about 3 nm. The periodic, molecular-scale image was superimposed on the hills and valleys. The Nanoscope II contains a '2D fast Fourier transform filter' which can

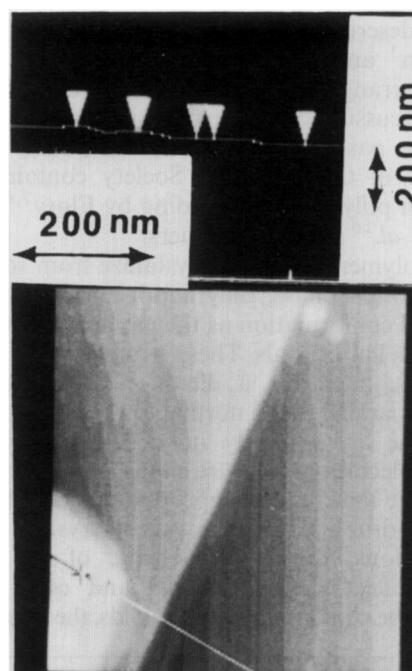


Figure 2 A line section perpendicular to the growth edge shows the crystal thickness of the steps. The thickness of the basal lamella is 11.5 nm and the top layer in the growth spiral is 10.44 nm thick

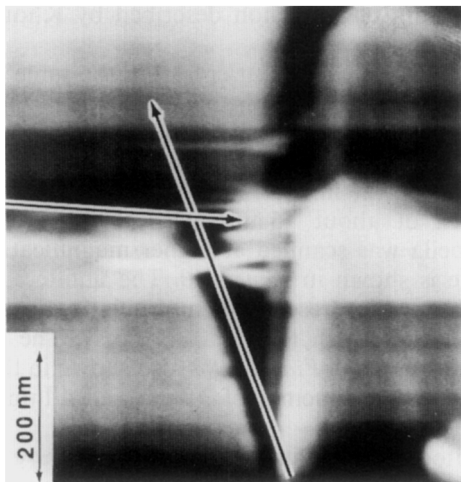


Figure 3 The lower left corner shows part of a lamellar crystal with $\{110\}$ growth faces indicated by the arrows. A fold domain boundary is present along the b axis of the crystal

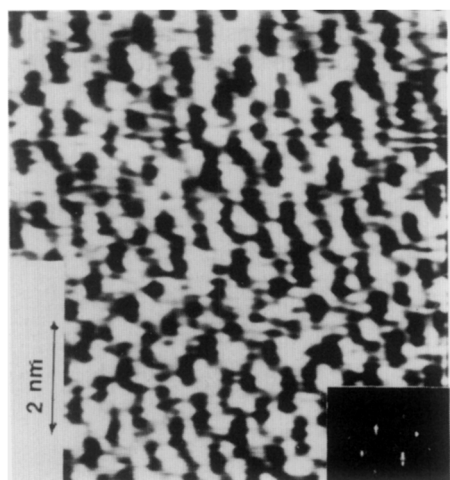


Figure 4 An area of about 100 nm^2 from the lower fold domain of *Figure 3*. The fast Fourier transform is shown in the inset

adjust the average value of each scan line to that of the preceding line. This filter effectively removed the hills and valleys and produced images such as that shown in *Figure 4*. In *Figure 4*, the dominant rows of high points are parallel to the growth face represented by the arrow running from the base of *Figure 3* towards the upper left. This parallelism indicates that these rows of high points correspond to successive fold planes in the crystal. The highest points in these rows are separated by 0.89 nm . This is the repeat distance of folds in the $\{110\}$ fold planes of hollow pyramidal crystals. The inset in *Figure 4* shows the fast Fourier transform of the image. Six intense diffraction spots were observed. *Figure 5* was created by transformation of the intensities near these diffraction spots back to an image which emphasizes the directions and primary spacings deduced from the original image.

The interpretation of the other distances observed in *Figure 5* is complicated. Polyethylene crystals grow in a hollow pyramidal or tent-like form. Neighbouring fold planes are displaced in the $[001]$ direction with respect to each other. The displacement can be by n repeat distances along the crystallographic c axis (case 1) or by $(n+0.5)$ repeat distances (case 2)¹⁸. This displacement avoids having the bulky folds side by side in the same

(001) plane. In the uncollapsed pyramid, the stems of the folded molecules are perpendicular to the base plane of the pyramid. When the pyramid collapses so that the lamellae lie flat on the substrate, the molecular axes are generally rotated away from the perpendicular direction.

Many possible local deformations and rotations of the region shown in *Figure 3* might have occurred during the collapse of the hollow pyramid. A probable collapse, for a small region near a growth face, involves rotation, with no local deformation, of the lamellae around a line parallel to the intersection of a $\{110\}$ fold plane and a $\{332\}$ plane to which the folds are tangent in the uncollapsed crystal (case 2, $n=1$). For this kind of rotation, the repeat distance of the folds along the directions parallel to the rotation axes remains invariant, while the separation between the folds in all other directions, when viewed from a direction perpendicular to the $\{332\}$ planes, depends on the amount of rotation. For this collapse mode the separation between rows of folds in a fold plane, measured in a direction perpendicular to the row and lying in a $\{332\}$ plane, is 0.48 nm for case 1 crystals with $n=1$. For case 2 crystals, the distance is 0.58 nm for $n=1$. The value of $n=1$ for a case 2 crystal corresponds to a displacement of adjacent fold planes by $1.5c$, which is a three-carbon displacement of the fold planes. This distance can be measured in both *Figures 4* and *5*, and is found to be 0.58 nm .

A sketch of the arrangements of folds in a case 2 crystal with $n=1$ when viewed along the perpendicular to a $\{332\}$ face of the pyramidal crystal is shown in *Figure 6*. *Figure 7* is an overlay of the filtered data of *Figure 5* and the diagram of *Figure 6* drawn to the same scale. The spacings in the data and the diagram agree to better than 10% in all directions.

A case 2, $n=1$ crystal might have grown at the time the crystals were formed or, less likely, it might have been created by mechanical deformation during collapse of a pyramidal crystal, or by forces exerted by the tip during scanning.

Figure 8 emphasizes the top 0.1 nm of the folds. The rows of folds in a single fold plane are nearly vertical in this 3D projection. There are several places where nearly horizontal folds (short, nearly horizontal lines) appear to connect stems in adjacent fold planes rather than their

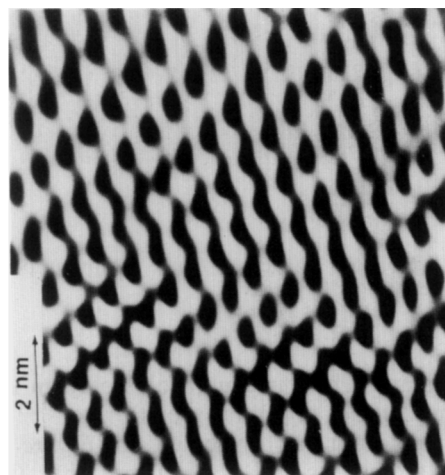


Figure 5 Transformation of the intensities near the diffraction spots in *Figure 4* to produce an image that emphasizes the directions and primary spacings

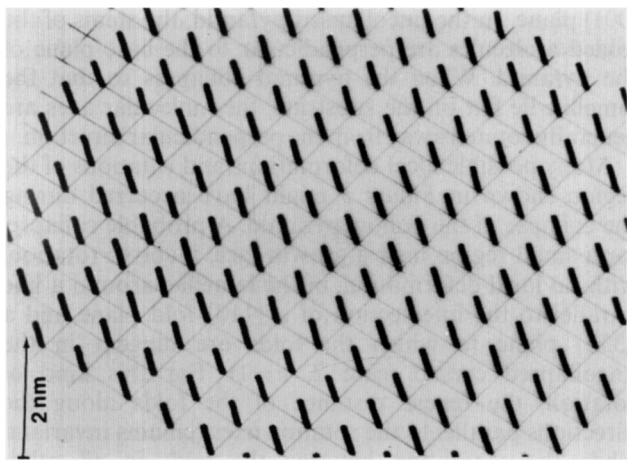


Figure 6 A sketch of a case 2 pyramid with $n=1$ collapsed by rotation around a line at the intersection of the $\{110\}$ growth planes and $\{332\}$ planes, viewed from a direction perpendicular to the $\{332\}$ planes

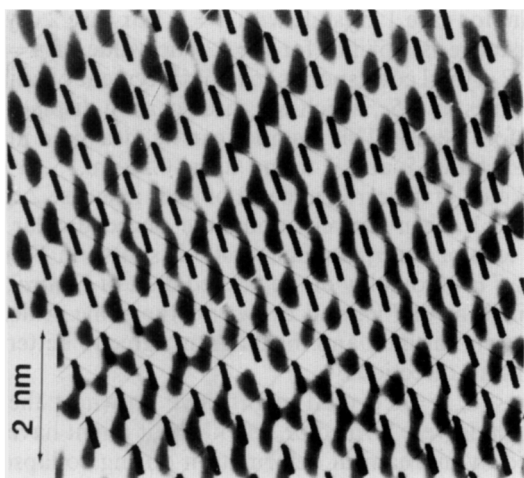


Figure 7 Figure 6 overlaid on Figure 5 to compare the two images

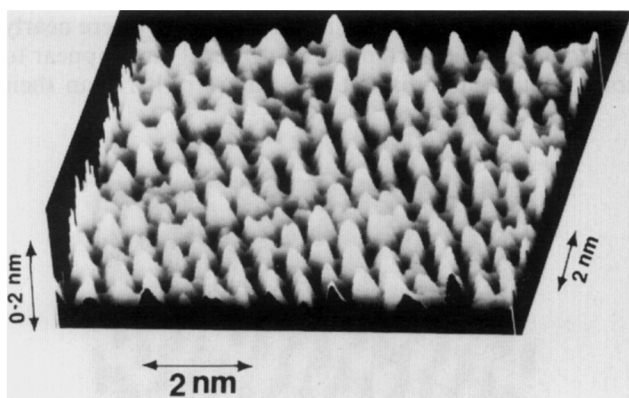


Figure 8 A projected 3D view of Figure 5 showing possible chain crossovers between $\{110\}$ planes

own fold plane. These irregular folds play an important role in the theories of crystal growth rate¹⁹⁻²¹.

The same data, as presented in Figure 5, show the same crossovers and also suggest that there may be small domains in which the folds are oriented differently from in the overall crystal. This possibility was suggested by Burbank²². It arises in connection with the

microsectoring phenomenon described by Khoury and Passaglia²³.

Figure 9 shows a different crystal in the same sample. A growth face runs across the area observed, from upper left to lower right. The basal lamella is 11.5 nm thick. Growth spirals are also seen on this crystal in the lower right corner of the image.

An area of about 15 nm^2 near the centre of the basal lamella was scanned at higher magnification and the image is shown in Figure 10. The unfiltered image clearly shows the presence of molecular-scale periodic features, even though the data are noisy. The 2D fast Fourier transform of Figure 10 is also shown in the inset, which shows line spacings of 3.9 nm and 4.1 nm in the image.

The autocorrelation image is shown in Figure 11. The prominent spacings in this image correspond to those expected for a collapsed crystal with monoclinic unit cell packing²⁴. The presence of a different crystal form can be rationalized by assuming that some crystals grew in the monoclinic form, or that a phase transformation to a monoclinic type III unit cell occurred in some crystals of this sample, or that a transformation took place during collapse or in response to stress created from the AFM tip.

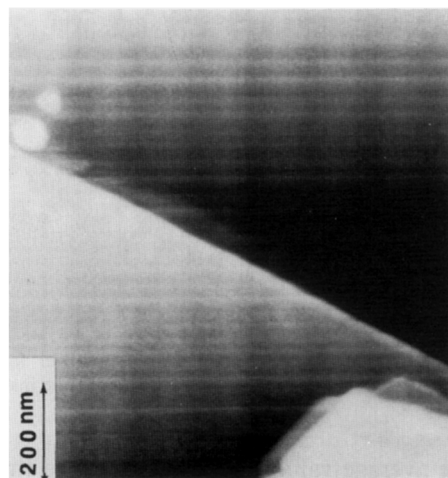


Figure 9 Top view of another crystal

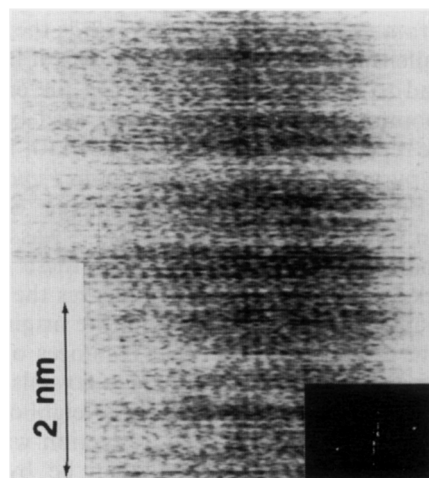


Figure 10 An area of 15 nm^2 near the centre of the basal lamella in Figure 9, showing raw data. The Fourier transform is shown in the inset

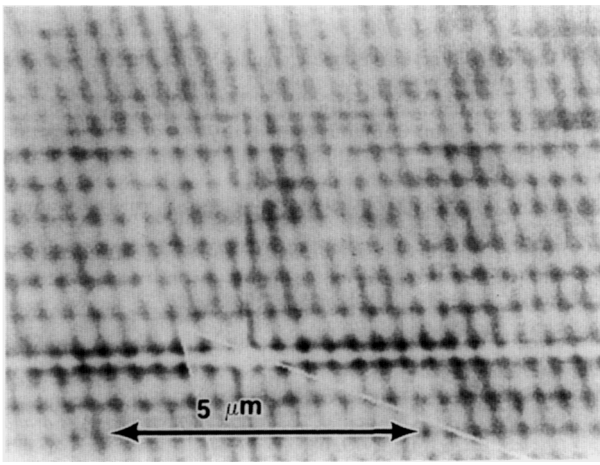


Figure 11 Autocorrelation image calculated from the data shown in Figure 10

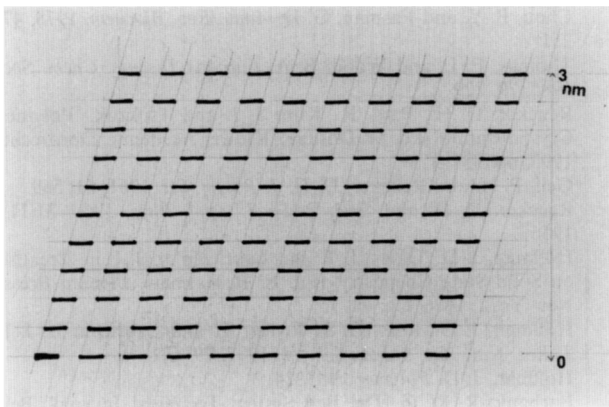


Figure 12 A sketch of a fold facet of a pyramid with a monoclinic type III unit cell with every adjacent $\{101\}$ plane displaced by one b repeat unit along the stem section, viewed along the perpendicular to a $\{111\}$ plane

Monoclinic type III unit cell packing²⁴ with a shift along the chain axis of one b repeat unit (the chain axis is along the b axis) in every adjacent $\{101\}$ plane is sketched in Figure 12 as viewed along the perpendicular to a $\{111\}$ plane. Figure 11 was overlaid with Figure 12 and the result is shown in Figure 13. The spacings in the data and the diagram agree to better than 10% in all directions.

DISCUSSION

The above paragraphs describe observations of folds in some of the polyethylene lamellar crystals that were examined. The data presented here are only from areas that could be shown to be on a fold surface by observation of a combination of features such as growth faces, the thickness of the lamellae, vertices of lozenge-shaped crystals and fold domain boundaries. Data of similar quality were obtained from several crystals and with at least two tips. The regular features observed fit the dimensions of known crystallographic forms of polyethylene, assuming that the surface to which the folds are tangential was viewed from a direction perpendicular to that surface. Since the chains are not perpendicular to the lamellae, the usual crystallographic dimensions

are not observed directly. The excellent quantitative agreement of the experimental data and those expected if the lamellae observed were simply lying flat on the substrate provides convincing evidence that the high spots observed show the locations of the folds. Local departures from the general arrangement, such as areas containing folds connecting stems in adjacent fold planes, were also observed. These areas are sometimes as small as one or two folds, and sometimes involve areas of 10 or 20 folds. These observations indicate that the imaging process had subnanometre lateral resolution and was not a process that resulted from a periodic tip on a periodic crystal, which cannot produce such small, singular features.

Images were obtained from other polyethylene crystals which showed periodic arrays with unfamiliar dimensions. This observation suggests that other combinations of rotation and deformation also occurred. In many attempts to observe folds on other polyethylene crystals from the same preparation and from other preparations, the images obtained were of much lower quality. In general, only randomly oriented molecular-scale features were observed. No long-range crystallographic order was apparent. A possible reason is that several areas on the tip touched the sample simultaneously. For example, the convolution of a small fraction of the folds protruding above the fold plane by one or two repeat units with a tip that had the shape of one atom protruding from a surrounding flat area with a diameter about equal to the separation between the protruding folds could produce images of the sort observed. At the other extreme, which ignores all the crystallographic and morphological evidence for regular folding, the images could also be produced by a sharp tip and a highly disordered surface such as would be expected from an amorphous polymer. Knowledge of the exact shape of the tip at the atomic scale would provide a great advance in our ability to attach meaning to such images. The smaller forces that can be used when the tip and the sample are immersed in liquid may improve AFM images. If the gradual development of protruding folds on the sample is occurring at room temperature, storage and observation of the sample at low temperatures should be helpful. More observations and correlations of morphology with growth condition, sample preparation and storage may also be helpful.

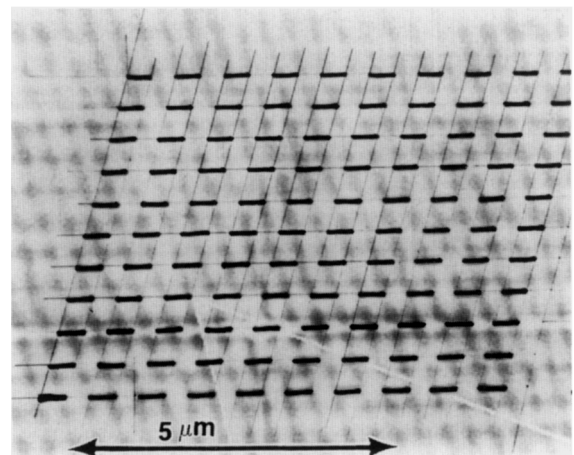


Figure 13 Overlay of Figure 12 on Figure 11 to show the comparison

CONCLUSION

Two sets of data in which the observation of arrays of folds is conclusive were presented. Repeat distances between folds in their own fold plane, which was identified by being parallel to a nearby growth face, were directly related to the crystal structure. In other directions, the observed distances between the folds were related to the crystallographic distances under the assumption that the region was deposited on the substrate by a simple rotation that brought the lamellae parallel to the substrate as the hollow pyramidal crystal collapsed.

The monoclinic crystal observed had a unit cell that has been reported to be a consequence of mechanical deformation of an orthorhombic crystal. This suggests that collapse of a hollow pyramid sometimes produces a crystallographic deformation. Alternatively, the monoclinic crystal regions may have grown in one of the more complicated crystals present in this sample, such as that shown near the upper right corner of *Figure 1*.

The possibility of observing singular structures at the scale of single folds in a large array of regular folds was demonstrated. Further observations of this sort will shed light on the proposed transformations between regimes¹⁹⁻²¹ of nucleation and growth that affect the growth rate.

The cases in which observation of a fold surface produced a disordered image are not interpreted. The convolution of blunt tips with irregularities on the surface could account for the disordered images. Protruding folds are an example, as are steps on the fold surface, one or two repeat units high, which are involved in the patches¹³ reported earlier.

ACKNOWLEDGEMENTS

We would like to thank the Edison Polymer Innovation Corporation (EPIC) and the National Science Foundation Center for Molecular and Microstructure of Composites (CMMC) for support.

REFERENCES

- 1 Geil, P. H. 'Polymer Single Crystals' Vol. 5, Interscience, New York, 1963
- 2 Bassett, D. C. in 'Principles of Polymer Morphology' (Ed. R. W. Cahn), Cambridge University Press, Cambridge, 1981
- 3 Mandelkern, L. 'Crystallization of Polymers', McGraw-Hill, New York, 1964
- 4 Wunderlich, B. 'Macromolecular Physics', Vol. 1, Academic Press, New York, 1973
- 5 Sanchez, I. C. *J. Macromol. Sci., Rev. Macromol. Chem.* 1974, **C10** (1), 113
- 6 Storks, K. H. *J. Am. Chem. Soc.* 1938, **60**, 1753
- 7 Flory, P. J. *Faraday Discuss. Chem. Soc.* 1979, **68**, 14
- 8 Yoon, Y. and Flory, P. J. *Faraday Discuss. Chem. Soc.* 1979, **68**, 288
- 9 Frank, F. C. *Faraday Discuss. Chem. Soc.* 1979, **68**, 7
- 10 Hoffman, J. D., Guttman, C. M. and DiMarzio, E. A. *Faraday Discuss. Chem. Soc.* 1979, **68**, 177
- 11 Walton, A. G. in 'Conformation of Biological Molecules and Polymers' (Eds E. D. Bergmann and B. Pullman), Vol. 5, Academic Press, New York, 1973, pp. 189-199
- 12 Cantor, C. R. and Schimmel, P. R. 'Biophysical Chemistry', Part 1, Freeman, New York, 1980
- 13 Creighton, T. E. 'Proteins, Structures and Molecular Properties', Freeman, New York, 1984, p. 99
- 14 Chou, P. Y. and Fasman, G. D. *Annu. Rev. Biochem.* 1978, **47**, 251
- 15 Thomas, E. L. and Wood, B. A. *Faraday Discuss. Chem. Soc.* 1985, **79**, 229
- 16 Reneker, D. H., Patil, R., Kim, S. J. and Tsukruk. 'Polymer Crystallization' (Ed. M. Dosière), Kluwer Academic, Dordrecht, 1993, pp. 357-373
- 17 Geil, P. H. and Reneker, D. H. *J. Polym. Sci.* 1961, **51**, 569
- 18 Reneker, D. H. and Geil, P. H. *J. Appl. Phys.* 1960, **31**(11), 1916
- 19 Hoffman, J. D., Davis, J. T. and Lauritzen Jr, J. I. in 'Treatise on Solid State Chemistry' (Ed. N. B. Hannay), Plenum Press, New York, 1976, Ch. 7
- 20 Hoffman, J. D., Ross, G. S., Frolen, L. and Lauritzen Jr, J. I. *J. Res. Natl Bur. Stand., Sect. A.* 1977, **79**, 671
- 21 Hoffman, J. D. *Polymer* 1983, **24**, 3
- 22 Burbank, R. D. in 'The Bell System Technical Journal', Bell Telephone Laboratories, Murray Hill, NJ, 1960, pp. 1627-1663
- 23 Khoury, F. and Passaglia, E. in 'Treatise on Solid State Chemistry' (Ed. N. B. Hannay), Vol. 3, Plenum Press, New York, pp. 335-496
- 24 Kiho, H., Peterlin, A. and Geil, P. H. *J. Appl. Phys.* 1964, **35**(5), 1599